E. coli 6S RNA release from RNA polymerase requires σ^{70} ejection by scrunching and is orchestrated by a conserved RNA hairpin

SHANKER SHYAM S. PANCHAPAKESAN and PETER J. UNRAU[1]
Department of Molecular Biology and Biochemistry, Simon Fraser University, Burnaby, British Columbia V5A 1S6, Canada

ABSTRACT

The 6S RNA in *Escherichia coli* suppresses housekeeping transcription by binding to RNA polymerase holoenzyme (core polymerase + σ^{70}) under low nutrient conditions and rescues σ^{70}-dependent transcription in high nutrient conditions by the synthesis of a short product RNA (pRNA) using itself as a template. Here we characterize a kinetic intermediate that arises during 6S RNA release. This state, consisting of 6S RNA and core polymerase, is related to the formation of a top-strand "release" hairpin that is conserved across the γ-proteobacteria. Deliberately slowing the intrinsic 6S RNA release rate by nucleotide feeding experiments reveals that σ^{70} ejection occurs abruptly once a pRNA length of 9 nucleotides (nt) is reached. After σ^{70} ejection, an additional 4 nt of pRNA synthesis is required before the 6S:pRNA complex is finally released from core polymerase. Changing the *E. coli* 6S RNA sequence to preclude formation of the release hairpin dramatically slows the speed of 6S RNA release but, surprisingly, does not alter the abruptness of σ^{70} ejection. Rather, the pRNA size required to trigger σ^{70} release increases from 9 nt to 14 nt. That a precise pRNA length is required to trigger σ^{70} release either with or without a hairpin implicates an intrinsic "scrunching"-type release mechanism. We speculate that the release hairpin serves two primary functions in the γ-proteobacteria: First, its formation strips single-stranded "−10" 6S RNA interactions away from σ^{70}. Second, the formation of the hairpin accumulates RNA into a region of the polymerase complex previously associated with DNA scrunching, further destabilizing the 6S:pRNA:polymerase complex.

Keywords: regulatory RNA; 6S RNA, RNA polymerase; scrunching; σ factor; conformational change

INTRODUCTION

Transcription of DNA into RNA by RNA polymerase is a fundamental and hence heavily regulated process in bacteria. Prior to transcription, *Escherichia coli* core RNA polymerase binds with nanomolar affinity to a σ factor that confers DNA promoter specificity to the enzyme (Sharma and Chatterji 2010). The housekeeping or σ^{70} holoenzyme (henceforth Eσ^{70}) opens the closed promoter via a three-step process that correctly positions the template strand in the polymerase active site (Chen et al. 2010). The NTP-dependent process of abortive initiation then deforms this static initiation structure into a processive elongation complex by "scrunching" the top and bottom template strands found in the open DNA promoter bubble into the polymerase via the synthesis of a DNA:RNA heteroduplex. This scrunching gradually adds strain energy to the overall complex and can accumulate ~14–18 kcal/mol (Kapanidis et al. 2006; Revyakin et al. 2006) once a DNA:RNA heteroduplex of ~9–13 bp has been synthesized (Chen et al. 2010). The scrunched polymerase triggers a global rearrangement of the complex into a processive structure. This relatively poorly understood process often, but not always, results in the profound weakening of σ^{70} binding (Mukhopadhyay et al. 2001; Zhilina et al. 2012), which can in turn be recycled for subsequent rounds of transcription.

The 6S RNA is a small noncoding RNA that plays a key role in regulating eubacterial transcription at the global level. One of the first noncoding RNAs to be sequenced (Brownlee 1971), it accumulates to a high level in stationary phase and regulates transcription by competitively binding to Eσ^{70} in the place of σ^{70}-dependent DNA promoters (Wassarman and Storz 2000). The resulting stable RNP complex precludes DNA-dependent transcription in

[1]**Corresponding author**
E-mail punrau@sfu.ca
Article published online ahead of print. Article and publication date are at http://www.rnajournal.org/cgi/doi/10.1261/rna.034785.112.

E. coli and inhibits all but the strongest σ^{70}-dependent promoters in vivo (Trotochaud and Wassarman 2004). When starving cells from stationary phase encounter rich nutrient conditions, a short product RNA (pRNA) templated by the 6S RNA itself is produced using the higher NTP levels made available by the beneficial environment that allows outgrowth (Wassarman and Storz 2000). This pRNA synthesis in turn triggers the ejection of the 6S:pRNA from RNA polymerase (Wassarman and Saecker 2006), allowing normal transcription of the σ^{70} housekeeping genes to resume. Thus the 6S RNA transcript, which is itself initiated by both σ^{70} and σ^{38} (stationary phase) promoters (Kim and Lee 2004), provides an elegant negative feedback mechanism to directly regulate the global cellular transcriptional state via complex interactions with RNA polymerase.

The 6S RNA resembles an open form DNA promoter (Fig. 1A) and binds to Eσ^{70} via interactions with specific regions of its sequence that correspond to parts of a σ^{70} DNA promoter (Barrick et al. 2005). A phylogenetically conserved "−35" region (Fig. 1A; Barrick et al. 2005) that is located upstream of the large open bubble structure has been demonstrated by in vitro selection, as well as truncation experiments, to be essential for 6S RNA binding to *E. coli* Eσ^{70} (Shephard et al. 2010). This site interacts with the C terminus of σ^{70} as deleting the 4.2 subdomain precludes 6S RNA binding (Klocko and Wassarman 2009). Since this region of the σ^{70} interacts with both the 6S RNA and the −35 DNA promoter element, a mechanism for the 6S RNA to competitively bind to Eσ^{70} is naturally suggested (Wassarman and Storz 2000; Shephard et al. 2010). A poorly conserved bulged helix in the 6S RNA spaces this −35 binding element away from a large open bubble that contains a "−10" region that is highly conserved in the γ-proteobacteria (Barrick et al. 2005; Shephard et al. 2010).

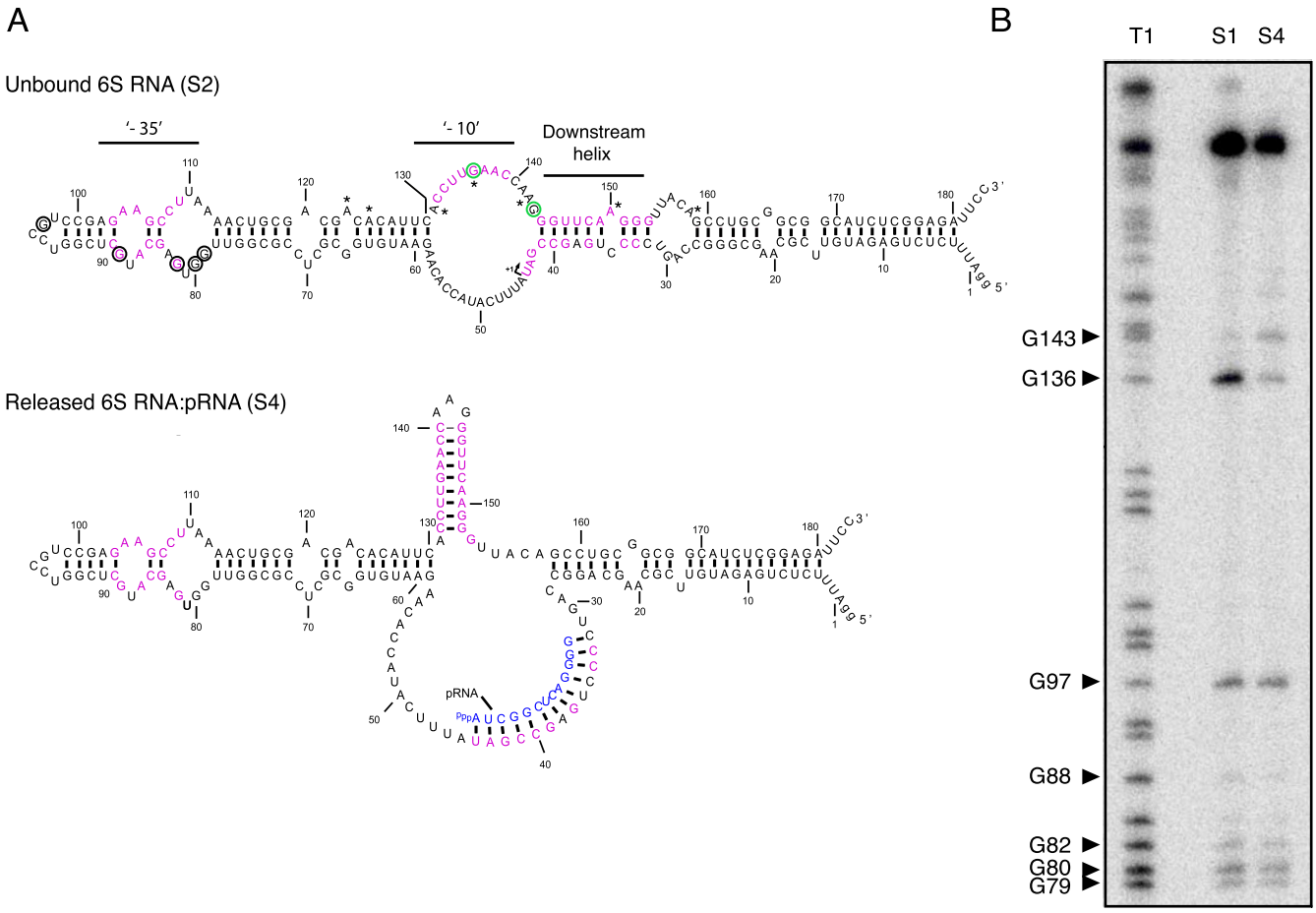

FIGURE 1. Presence of hairpin in the released 6S:pRNA complex. (*A*) Highly conserved residues in the unbound 6S RNA (S1 state) from γ-proteobacteria are shown in purple. pRNA is shown in blue. The hairpin forms in the released 6S RNA:pRNA complex (S4 state) between the phylogenetically conserved "−10" region and the top strand of the downstream helix. Green circles indicate G residues that change their protection pattern upon release, while black circles indicate single-stranded G residues that are unaffected by the release process. Residues previously shown to form UV crosslinks with holoenzyme in the bound Eσ^{70} (S2 state) are marked with asterisks (Gildehaus et al. 2007). (*B*) Native T1 RNase digestion of 5′ ^{32}P end-labeled 6S RNA before binding (S1) and after pRNA induced release (S4). Analyzed using 10% denaturing PAGE. T1 indicates denaturing T1 RNase digest of the 6S RNA unbound construct.

This region, would by geometric analogy to the −10 DNA promoter recognition element (Barrick et al. 2005), make interactions with σ^{70} regions 2.3 and 2.4 and potentially region 3 (Murakami et al. 2002). Consistent with this picture, mutating the −10 region can either increase or decrease 6S RNA binding and has been shown to modulate 6S RNA release rate (Shephard et al. 2010). The conserved downstream region has only a marginal influence on the initial binding of the 6S RNA to Eσ^{70}. Notably in the γ-proteobacteria, the top strand of this region is the exact reverse complement of the −10 region. Therefore, when pRNA invades into the downstream helix by base-pairing to the bottom strand, the complementary top strand, which would now be unpaired, can potentially base pair with the conserved −10 region, forming a stem–loop (Fig. 1A). Together, these data suggest a potential role for the formation of a "release" hairpin during 6S RNA release from Eσ^{70} in the γ-proteobacteria.

The pRNA-dependent formation of this potential hairpin structure is only predicted for bacteria that either are in or are closely related to the γ-proteobacteria. *Helicobacter pylori*, a member of the ε-proteobacteria, has such a potential hairpin, while the 6S RNAs from members of the α- and δ-proteobacteria do not make appropriate downstream pairing interactions with their −10 sequence (Barrick et al. 2005). Interestingly, phylogenetic evidence suggests that smaller preformed hairpins in the −10 region are quite common in other eubacteria. The 6S-1 RNA in *Bacillus subtilis*, for example, appears to have such a preformed hairpin in the −10 region and, when hybridized to a synthetic pRNA, undergoes significant secondary-structure rearrangements between the downstream duplex and the template strand of the open RNA bubble (Beckmann et al. 2012). These rearrangements leave the preformed hairpin structure found in the −10 region invariant before and after pRNA hybridization in contrast to the potential hairpin formation mechanism predicted in the γ-proteobacteria. Such variations suggest the existence either of several distinct 6S RNA release mechanisms or a polymerase-dependent mechanism that is itself exploited by a set of distinct 6S RNA secondary-structure rearrangements that span the eubacteria.

In support of the second hypothesis, we show that a hairpin structure formed between the −10 region of the γ-proteobacteria 6S RNA and the top strand of the downstream duplex in the course of pRNA synthesis helps to coordinate first the release of σ^{70} and then, in a second pRNA-dependent step, the ejection of the 6S:pRNA complex from core polymerase. Remarkably, we find that removing the hairpin delays both steps in this process but does not change the progression of the 6S RNA release process or the sharp nature of these transitions as pRNA extension proceeds. The abruptness of these transitions indicates that a universal mechanism, similar to that of scrunching during the transition from transcriptional initiation to elongation, exists for 6S RNA release across all eubacteria.

RESULTS

6S secondary-structure rearrangement upon pRNA induced release

We find evidence for a total of four distinct structural states during pRNA-induced 6S RNA release in *E. coli*. The unbound 6S RNA (S1 state) and the final released 6S:pRNA complex (the S4 state) are devoid of protein and provide simple evidence that a structural rearrangement occurs during the process of 6S RNA release from *E. coli* RNA polymerase. Having shown that the −10 region can alter both binding and release rate (Shephard et al. 2010), we noticed together with others (Wurm et al. 2010; Beckmann et al. 2012), that the top strand of the conserved downstream helix is complementary to the conserved −10 region (Fig. 1A). Although this hairpin forming potential has been noticed previously, there has been no evidence to date that this hairpin actually forms during 6S RNA release, and hence, the importance of this release hairpin is unknown. We hypothesized that the 6S RNA, after binding holoenzyme to form the bound S2 state, could potentially form a hairpin as a consequence of pRNA synthesis that would preclude binding interactions between the −10 region and σ^{70}. G136, which makes a UV crosslink to the holopolymerase in the S2 state (Fig. 1A; Gildehaus et al. 2007), is predicted to be unpaired in the unbound central bubble of the 6S RNA and should become strongly protected against T1 RNase digestion upon formation of a 6S RNA hairpin as T1 RNase cuts only unpaired G residues. Indeed, T1 RNase digestion of the free 6S RNA (S1) under native conditions revealed G136 to be sensitive to T1 RNase (Fig. 1B), consistent with previous secondary-structure models of the 6S RNA (Barrick et al. 2005; Shephard et al. 2010). After binding and then releasing the 6S RNA from the holoenzyme via pRNA synthesis so as to form the S4 state, G136 became significantly resistant to T1 RNase while the cleavage pattern of G97, G88, G82, G80, and G79, which were not expected to undergo any secondary-structure rearrangement, remained unaffected. G143, adjacent to the initial base pair of the downstream duplex in the free S1 state, became more sensitive to T1 RNase in the S4 state, as would be expected if found in the proposed hairpin triloop after formation of the 6S RNA hairpin (Fig. 1A). Having established this important change in secondary structure between the S1 and S4 states, we next explored potential intermediate states of the release process that could depend on pRNA length.

6S:pRNA:E release intermediate found between bound (S2) and final released state (S4)

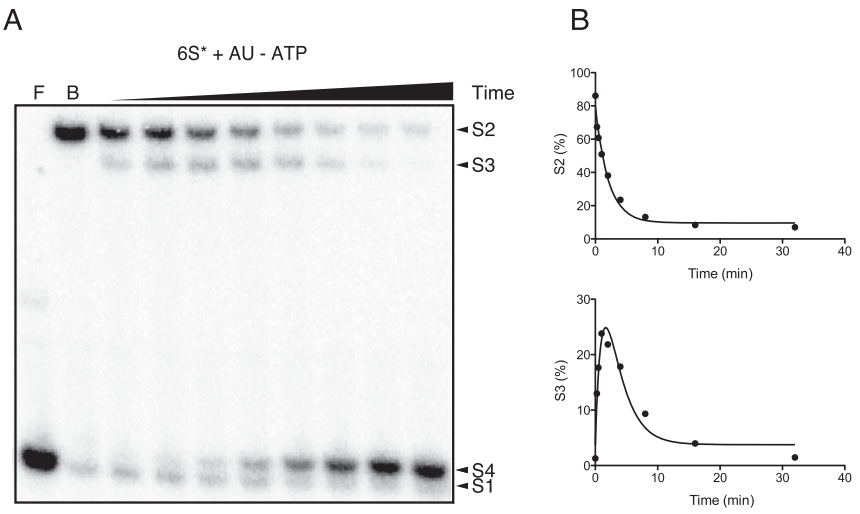

FIGURE 2. A 6S:pRNA:Eσ^{70} intermediate state (S3) revealed by nucleotide feeding experiments. (*A*) Native gel analysis of ^{32}P body-labeled 6S RNA (6S*) showing the emergence and decline of the S3 state when pRNA synthesis is initiated with AU dinucleotide (GTP concentration 25.9 μM, ATP withheld). Time points are 0.25, 0.5, 1, 2, 4, 8, 16, and 32 min. F indicates free 6S* (S1); B, bound Eσ^{70} complex (S2). (*B*) Fitted data for the S2 and S3 state kinetics shown in panel *A* (for fitting details, see Materials and Methods) using Supplemental Equations 4 and 5, respectively.

The bound 6S:Eσ^{70} (S2) complex is capable of being very rapidly released both in vitro and in vivo (Wurm et al. 2010). By use of aggressive release conditions that simulate the early stages of outgrowth from stationary phase (3.75 mM $MgCl_2$, 148 μM of each NTP, and stoichiometric amounts of heparin), the 6S:pRNA complex can be released from RNA polymerase with a half-time of ~50 sec and produce a 6S:pRNA complex containing a pRNA that is 13 nucleotides (nt) long (Supplemental Fig. S1). Titrating magnesium has a dramatic effect on release rate but leaves the length of the pRNA invariant. We believe that addition of heparin during binding and 6S RNA release simulates the nonspecific interactions of endogenous RNA during the release process and results in the in vitro production of pRNAs that are very comparable in size to that observed in vivo. In the absence of heparin, pRNA sizes increase (Supplemental Fig. S2) but appear to have limited in vivo significance; as pRNAs of length ~10–14 nt are known to be produced within 15–30 sec of rapid outgrowth in *E. coli* (Wurm et al. 2010) and are very similar in size to the pRNAs observed in *H. pylori* (12 nt long) (Sharma et al. 2010) and *B. subtilis* (8–12 nt long) (Beckmann et al. 2011). Longer RNAs complementary to a pRNA probe have been detected by Northern blot from *E. coli*, but they start to accumulate only after 1–2 min of outgrowth (Wurm et al. 2010). Such RNAs could reflect the rapid in vivo degradation of the 6S RNA itself, or alternatively, longer pRNAs could have a role secondary to the initial and very rapid burst of short pRNAs synthesis observed at the start of outgrowth. Both in vivo and in vitro, the high intrinsic speed of the 6S RNA release process has made it difficult to explore the potential release intermediate states.

In order to slow down the 6S RNA release process, pRNA synthesis conditions were modified. By use of AU dinucleotide (25 μM) to initiate RNA synthesis (Wassarman and Saecker 2006), we found that removing ATP results in a new intermediate state between the S2 and S4 states. Analysis by native gel revealed the conversion of the S2 state into a new intermediate state (S3) that initially grows and then declines as the S2 state is depleted and the S4 state is produced (Fig. 2A,B). A simple two-step kinetic model (see Supplemental Equations 1–6), where the S2 state proceeds to state S3 with a first-order rate k_{23} and then from state S3 to state S4 with a rate k_{34}, fits acceptably to the S3 state time-course data (Fig. 2B) and gave $k_{23} = 0.36 \pm 0.04$ min^{-1} and $k_{34} = 0.94 \pm 0.11$ min^{-1} under the slow pRNA synthesis conditions used for this assay. An independent fit to the S2 kinetics gave for this experiment $k_{23} = 0.48 \pm 0.07$ min^{-1}. While the k_{23} values were not in perfect agreement between the S2 and S3 fits, it is notable that the S2 state data did not fit perfectly to a single exponential, suggesting that the S2 state is not completely homogeneous and that it contains a subpopulation (we estimate 10%–15% for our enzyme) that releases slower and/or incompletely relative to the majority species. If this subpopulation does not utilize the S3 state during release, the increased k_{23} value determined for the S2 fit relative to the S3 fit could potentially be explained.

If all steps of this 6S RNA release process are pRNA-dependent, then the length of the pRNA in the S2, S3, and S4 states should be in strict and increasing progression. Tracking pRNA-induced release by labeling AU with γ-[^{32}P]-ATP and polynucleotide kinase revealed no evidence for pRNA in the S2 state, whereas bound 6S RNA is clearly evident (Fig. 3A). The S3 state contained both 6S RNA and a shorter 9-nt-long pRNA (Fig. 3A,B). This was initially unexpected as pRNA synthesis initiated with AU in the absence of ATP requires ATP for the ninth pRNA addition against template residue U36 and should therefore only contain an 8-nt pRNA. If, however, *E. coli* RNA polymerase can add GTP to form a wobble pair across from U36, then the observed pattern of extension makes complete sense (the wobble pair could delay pRNA extension) and implies that the S3 state and its 9-nt-long pRNA are indeed intermediate to the S2 and S4 states. Further support for this model was found by titrating GTP. Our

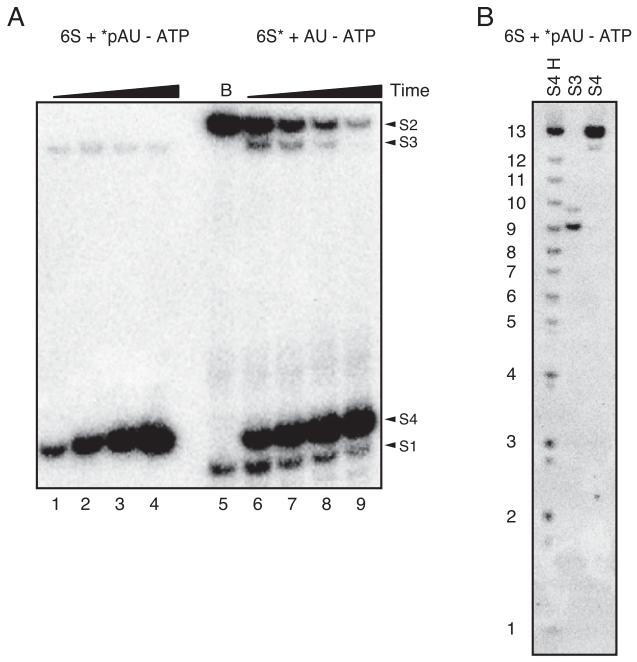

FIGURE 3. pRNA is present in the S3 and S4 states of the 6S RNA release complex. (*A*, lanes *1–4*) Time course using ^{32}P radiolabeled AU (*pAU) dinucleotide, time points 2, 5, 10, and 30 min. (*A*, lanes *6–9*) ^{32}P body-labeled 6S RNA (6S*) showing bound (S2) complex followed by the emergence of the S3 and S4 states after addition of 25 μM AU, 147 μM of each CTP, GTP, and UTP. B indicates bound Eσ^{70} complex (lane *5*). (*B*) Size characterization of *pAU-labeled pRNA extracted from the S3 and S4 states. Recovered RNA was analyzed using 23% denaturing PAGE. S4 H indicates alkaline hydrolysis ladder of the S4 state pRNA.

two-state model predicts that GTP concentration should have a pronounced effect on the k_{34} rate constant as four subsequent GTP additions are required to convert the 9-nt-long pRNA in the S3 state to the 13-nt-long pRNA found in S4 state. As predicted, increasing GTP concentration decreased the amount of S3 state observed (Supplemental Fig. S3). In no conditions tested did we observe a change in pRNA size within either the S3 or the S4 states; they always remained at 9 nt and 13 nt, respectively.

The S3 band migrates with a mobility previously attributed to 6S RNA bound to core polymerase (Wassarman and Saecker 2006; Wurm et al. 2010). To confirm that the S3 state is devoid of σ^{70}, a native gel supershift assay with mouse monoclonal anti-σ^{70} antibody (Neoclone) was performed. Adding σ^{70} antibody prior to the initiation of pRNA-dependent release resulted in a supershift of the S2 band (Fig. 4A). The addition of anti-σ^{70} antibody during 6S RNA:holoenzyme complex release using the AU–ATP nucleotide feeding approach did not affect the S3 band mobility (Fig. 4B). Simultaneously, the addition of the antibody lowered both the overall 6S RNA release rate and the amount of S3 state observed (Fig. 4B; Supplemental Fig. S4). This would be predicted if the anti-σ antibodies bind to σ^{70} in the S2 state, so as to lower the pRNA-dependent rate constant k_{23} from state S2 to S3, but not the rate constant k_{34} out of S3 and into S4 (where we presume that owing to the absence of σ^{70}, the antibody would no longer have an inhibitory effect on the S3 to S4 state kinetics).

Removing 6S RNA hairpin does not preclude σ^{70} ejection

In order to further understand the role of the hairpin formation in the release process, a 6S RNA variant, 6S_S, was made by swapping the top and bottom strand of the downstream helix so that the hairpin could not be formed (Fig. 5A). This construct leaves the pRNA initiation site unchanged, as well as the stability of the downstream helix largely invariant. On comparing the release kinetics of the 6S and 6S_S RNAs, we saw that the 6S_S RNA construct releases at least 10 times slower than the wild-type 6S RNA under aggressive release conditions. Whereas the 6S RNA is fully liberated in under 2 min, the 6S_S is still forming the S4 state after 10 min of incubation (Fig. 5B; Supplemental Fig. S5). Intriguingly, the prominent emergence of the S3 intermediate-state band implied that the 6S_S construct could still trigger the rapid release of σ^{70} while requiring a longer time to convert the S3 state, so formed, to the S4 state.

Not only did the 6S_S RNA eject σ^{70} prior to release, but it also produced a S3 state containing pRNA dominated by a specific size of pRNA. Whereas the 6S RNA produced a pRNA 9 nt in length in the S3 state using modified NTP feeding conditions, the 6S_S, when released with high magnesium (3.75 mM), and all four NTPs produced a pRNA distribution that was nearly completely dominated by a 14-nt-long pRNA (Fig. 5C). Just as for the 6S RNA, no evidence for pRNA in the S2 state was observed (Supple-

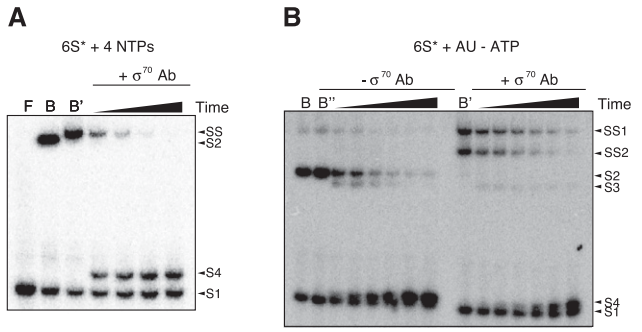

FIGURE 4. Anti-σ^{70} antibody supershift assay showing S3 state is devoid of σ^{70}. (*A*) 25 nM radiolabeled 6S RNA bound to 200 nM holoenzyme was incubated with mouse anti-σ^{70} antibody and was released with 147 μM of each NTP and 3.75 mM $MgCl_2$. F indicates free 6S; B, bound Eσ^{70} complex; B′, Eσ^{70} Ab; and SS, super shifted band. Time points of 2, 4, 8, 16, and 32 min were loaded in a 5% native gel with 5% glycerol. (*B*) The 25 nM body-labeled 6S RNA bound to 200 nM holoenzyme was incubated with or without mouse anti-σ^{70} antibody as indicated and was released with 147 μM of each CTP, GTP, and UTP; 1.5 mM $MgCl_2$; and 25 μM AU. Time points of 1, 2, 4, 8, 16, and 32 min were loaded as in panel *A*.

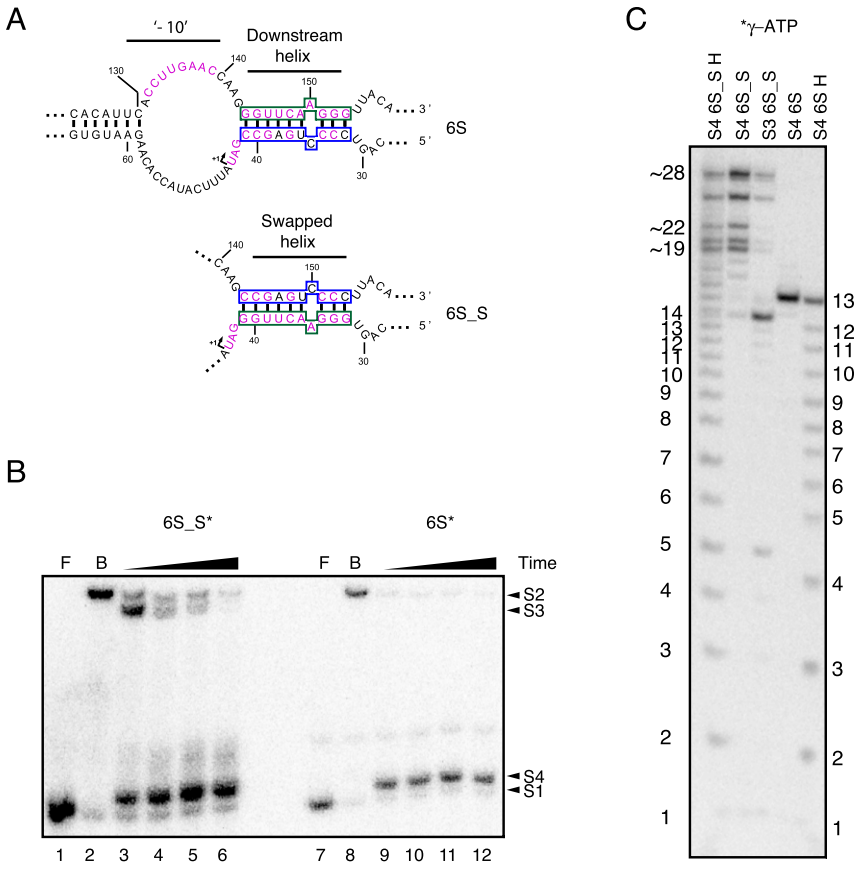

FIGURE 5. Abolishing the 6S RNA hairpin increases pRNA length and release time. (*A*) The 6S RNA swapped construct (6S_S) conserves pairing interactions in the downstream region but lacks the ability to form a hairpin. The top strand in the 6S RNA (green box) was swapped with the bottom strand (blue box) to generate the 6S_S construct. (*B*) Radiolabeled 6S_S (6S_S*) release assay showing a dramatic accumulation of the S3 state. (Lanes *1–6*) 6S_S RNA. (Lanes *7–12*) 6S RNA. Time points are 2, 5, 10, and 30 min; F indicates free RNA; B, bound RNA. (*C*) pRNA lengths in the S3 and S4 states of 6S_S relative to 6S RNA S4 state. All pRNAs were initiated with γ−[^{32}P]-ATP. H indicates alkaline hydrolysis ladder. Samples were analyzed using 23% denaturing PAGE.

mental Fig. S6). The pRNAs found in the released 6S_S RNA S4 complex, in contrast to the S3 state, were no longer homogeneous. At least five distinct sizes were observed, with the shortest being 18 nt long and the longest being ~28 nt long (Fig. 5C). These RNAs were all found to have related sequence as the hydrolysis ladder for the entire set of bands produced a homogenous set of bands. The two longest pRNA bands are dominant in the S4 state (22× the signal seen for the 14-nt-long pRNA band) but are also seen weakly in a complex having a mobility very similar to that of the S3 state (the two longer bands have 0.64× the signal seen relative to 14-nt band in the excised S3 state pRNA). These data together imply that these longer pRNAs can form rapidly after σ^{70} ejection but do not immediately trigger 6S_S:pRNA release from core polymerase, in distinct contrast to 6S RNA release when hairpin formation was possible. As expected in the aggressive release conditions used for the 6S_S RNA release, the wild-type 6S RNA did not manifest an obvious S3 band but did robustly convert the S2 state to S4 state (presumably with an unobserved S3 transient intermediate), with the S4 state containing a pRNA of 13-nt size (Fig. 3B) consistent with our previous observations using altered nucleotide release conditions.

DISCUSSION

During pRNA synthesis in the γ-proteobacteria, a secondary-structure rearrangement occurs involving the phylogenetically conserved regions of the 6S RNA that results in the formation of a hairpin in the top strand of the 6S RNA. This hairpin forms once pRNA invasion destabilizes the downstream duplex sufficiently to allow the top strand to pair with the −10 sequence region. We have demonstrated that when pRNA synthesis is slowed, a pRNA precisely 9 nt long is sufficient to trigger the abrupt formation of the S3 state, which lacks σ^{70}. This length of pRNA appears to be important for two reasons: First, a 9-nt pRNA is precisely that required to make all top-strand residues of the conserved downstream helix (Fig. 1) available to pair with the conserved −10 region. Second, once a 9-nt pRNA has been synthesized, the polymerase active site is now located precisely at the start of a downstream bubble (defined by UUACA, residues 154–158 on the top strand, and CAGU, residues 28–31 on the bottom strand). This bubble could in principle facilitate the abrupt movement of the now unpaired top-strand residues of the downstream helix with respect to the polymerase active site and allow these residues to pair with the −10 region so as to form the release hairpin.

Hairpin formation strips the 6S RNA −10 sequence away from protein contacts in σ^{70} so as to destabilize σ^{70} binding to the 6S:pRNA:E complex. This interpretation is consistent with the phenotypes of a number of −10 sequence mutants that manifest release defects (Shephard et al. 2010). A C132A mutant introduces a net increase in S2 state binding and exhibits a significant release defect after addition of NTPs. This mutation destabilizes the 6S RNA hairpin by one terminal base pair, and since it binds initially more tightly to Eσ^{70} than wild-type 6S RNA, its phenotype is as expected if the formation of the weakened hairpin has difficulty competing for a stronger −10:protein interaction. Conversely, a U134A mutant decreases S2

binding but also releases more rapidly than wild-type 6S RNA. This would be expected if the bulged hairpin resulting from this mutation can still compete effectively for a weakened RNA:protein interaction. Together these two mutants support the idea that one function of hairpin formation is to destabilize interactions between the −10 region and $E\sigma^{70}$ that are initially present in the S2 bound state. Since the −10 region appears likely to make contacts specifically with σ^{70} (Murakami et al. 2002; Barrick et al. 2005; Shephard et al. 2010), we conclude that one important role of hairpin formation is to weaken 6S RNA interactions with σ^{70} and, hence, facilitate entry into the S3 state.

The 6S release process appears very similar to that of scrunching during transcriptional initiation. After σ^{70} ejection to form the S3 state, the 6S:pRNA complex is still firmly attached to core polymerase and survives entry into a native gel, implying that downstream interactions, which initially are quite weak in the S2 state (Shephard et al. 2010), are dramatically enhanced as a result of pRNA synthesis. The β′ jaw domain of the core polymerase is well known to play a critical role during transcriptional initiation and holds downstream dsDNA tightly as DNA is packed into the enzyme complex as a result of the ratcheting effect of NTP incorporation (Ederth et al. 2002). The jaw domain together with "hood" regions of the polymerase defined by the β and β′ subunits that define the top of a channel containing both the template and nontemplate stands appears likely to be fully envelope both the downstream and bubble regions of the 6S RNA. Since the 6S RNA is initially bound via its highly conserved −35 domain to the C terminus of σ^{70}, pRNA synthesis prior to formation of the S3 state could therefore be expected to the build-up strain inside the RNP complex that together weaken interactions between σ^{70} and the bound 6S:pRNA:core polymerase. This strain, as just discussed, is made more potent by the abrupt loss of −10 interactions that result from formation of the release hairpin. More critically, the formation of a hairpin in the −10 region would simultaneously "scrunch" RNA into a region of the holoenzyme complex that has previously been implicated in the accumulation of bulged ssDNA during the process of transcriptional initiation (Fig. 6; Revyakin et al. 2006). This interpretation is consistent with our findings that removing the hairpin does not prevent σ^{70} release or make the process less crisp, rather pRNA length increases by ∼5 nt so as create a 14-bp homoduplex at the moment of σ^{70} ejection. Such an observation fits naturally with a scrunching-type model, where additional ssRNA from both the top and bottom strands of the open 6S RNA bubble must accumulate inside the holoenzyme complex during pRNA synthesis in order to accumulate strain equivalent to that afforded by the release hairpin.

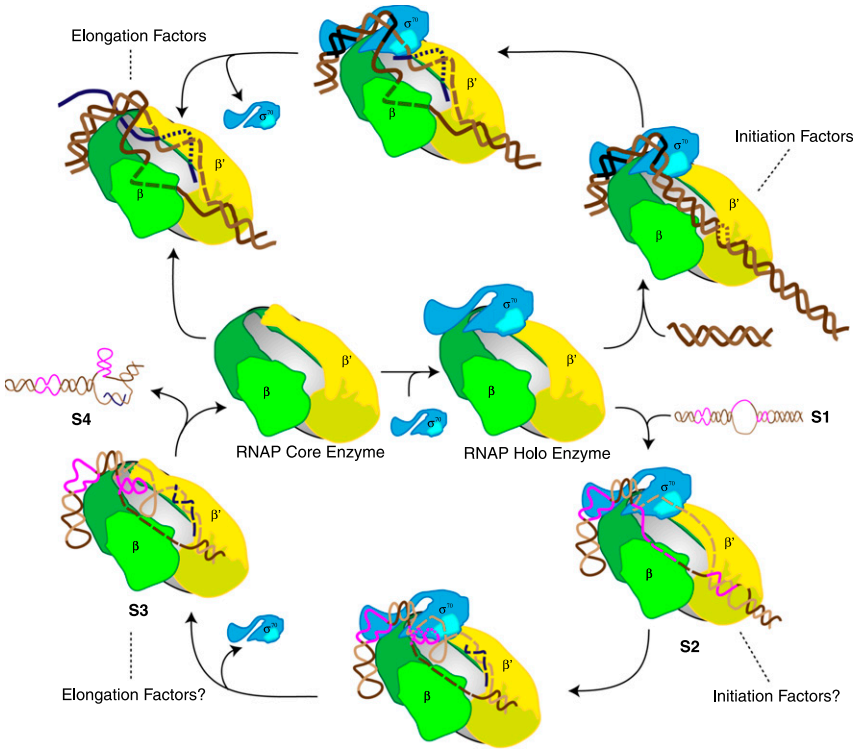

FIGURE 6. Model summarizing the major steps of *E. coli* 6S RNA release (*bottom*) relative to those of transcriptional initiation (*top*). Conserved sequence of 6S RNA in γ-proteobacteria is shown in purple; pRNA is in blue; and template strand is light brown and nontemplate is dark brown. Initiation and elongation factors have the potential to interact with and regulate 6S RNA release as indicated.

From an evolutionary perspective, release hairpin formation on the top strand of the 6S RNA open bubble of the sort found in *E. coli* 6S RNA occurs predominantly in the γ-proteobacteria (Shephard et al. 2010). In contrast, many eubacteria, such as *B. subtilis*, appear to utilize a smaller preformed hairpin in the top-strand −10 region (Supplemental Fig. S7). This preformed structure is correlated with an alternative secondary-structure pairing rearrangement between the bottom strand of the 6S RNA open bubble and downstream residues that become available during pRNA synthesis (Barrick et al. 2005; Beckmann et al. 2012; Cavanagh et al. 2012). These two distinct structural changes are both entirely consistent with the scrunching model just suggested for 6S RNA release in the γ-proteobacteria and suggest that this mechanism may be common to all eubacteria (Supplemental Fig. S7). Consistent with this, final pRNA sizes upon formation of the S4 state appear to be largely invariant (12–14 nt) across the eubacteria ob-

served in vivo to date (Sharma et al. 2010; Wurm et al. 2010; Cavanagh et al. 2012). Since the γ-proteobacteria form a top-strand release hairpin that simultaneously decreases −10 binding to σ^{70}, it would appear that these bacteria may be able to trigger 6S RNA release more abruptly than other eubacteria. This remains to be demonstrated, but it is a curious fact in this respect that the γ-proteobacteria are highly enriched in pathogens (i.e., the *Vibrionaceae, Enterobacteriaceae*, and the *Pseudomonadaceae*). An abrupt transition from stationary phase into rapid growth triggered by a 6S RNA release hairpin may be of considerable benefit to these organisms during the infection of a potential host.

More generally, the ejection of σ^{70} prior to 6S:pRNA release, summarized in Figure 6, offers the potential to study transcriptional initiation and its RNA-dependent regulation in a new light. If the S3 state can only be populated in certain cellular conditions, then two independent classes of transcriptional regulators normally thought to act on DNA:RNA polymerase complexes could act on the 6S RNA regulatory system in a variety of ways. The first class would interact with the bound S2 complex and modulate transcriptional initiation. The second class of regulators could act on the 6S:pRNA:E (S3) complex, which we presume would more closely resemble an elongation complex. Gre, NusA, and ppGpp, which are known to modulate elongation (Roberts et al. 2008), could have pronounced effects on the S3 state but would only be expected to be observed when the transition from S3 state to S4 state is rate limiting. Given that transcription and translation are tightly coupled events in bacteria, regulating the rate of S3-to-S4 conversion might be expected to be tied to translational regulation. We note that in this respect that the final conversion of the S3 to S4 state is dependent on GTP concentration and that GTP hydrolysis is integrally involved in EF-Tu–dependent ribosomal translational elongation. Equally exciting, pRNA-dependent 6S RNA release, with its many detailed parallels to transcription initiation, offers the opportunity to extract common mechanistic features shared between transcriptional initiation and RNA-dependent transcriptional regulation. These fundamental mechanisms are key to fully understand bacterial gene expression and regulation and promise to unify understanding of this important subject.

MATERIALS AND METHODS

DNA constructs

The 6S RNA gene was originally isolated from *E. coli* genomic DNA (Shephard et al. 2010). The 6S RNA swapped construct (6S_S) was made by PCR (10 mM TRIS at pH 8.3, 50 mM KCl, 1.5 mM $MgCl_2$, 0.1% gelatin, 200 μM each dNTP, 2.5 U/100 μL Taq polymerase, 0.5 μM primers), using P1, 5′-GAATCTCCGAGAT GCCGCCGCAGGCTGTAA*GGGGACTCGG*CTTGGTTCAAGGT, and P2, 5′-ttc taatacgactcactataGGATTTCTCTGAGATGTTCGCA AGCGGGCCAGT*GGGAACTTGG*GATATTTCATACCACAAGA. The lowercase residues indicate the T7 RNA polymerase promoter for in vitro transcription of the RNA; residues in italics are the regions of the inverted downstream helix.

6S RNA binding

We heated 25 nM ^{32}P body-labeled PAGE purified, T7 RNA polymerase in vitro transcribed 6S RNA for 2 min to 80°C, which was then cooled for 5 min to 50°C prior to binding to 200 nM *E. coli* RNA polymerase holoenzyme (Epicentre) in 15 mM HEPES (pH 7.5), 90 mM KCl, 0.75 mM DTT, 75 μg/mL heparin for 30 min at 37°C.

6S release

Aggressive release conditions

pRNA synthesis was initiated by the addition of 148 μM of each NTP and 3.75 mM $MgCl_2$ and incubation for 30 min at 37°C.

Modified release conditions

pRNA synthesis was initiated by the addition of 25 μM AU; 148 μM of each CTP, GTP, and UTP; and 3.5 mM or 1.5 mM $MgCl_2$ as indicated and was incubated for 30 min at 37°C. Reactions were quenched by the addition of 2× native gel loading dye containing 0.025% Bromophenol Blue and 0.025% xylene cyanol, 50% glycerol, 40 mM HEPES (pH 7.5), 120 mM KCl, 8 mM EDTA and loaded onto a 5% polyacrylamide gel with 5% glycerol ran with 1× TBE at 4°C.

T1 RNase digestion

5′-labeled 6S RNA was bound to Eσ^{70} and pRNA synthesis was initiated by adding NTPs and $MgCl_2$. For digestion in native conditions, T1 RNase was serially diluted in 20 mM HEPES (pH 7.5), 120 mM KCl, 50% glycerol and used to digest end-labeled 6S RNA so as to find optimal digestion conditions. Initial and released 6S RNA:pRNA complexes were added to the appropriate dilution of T1 RNase and incubated for 10 min at 50°C. In the case of denaturating T1 RNase digestion, the enzyme was diluted in 20 mM sodium citrate with 6 M urea. The reactions were quenched by adding a denaturating loading dye with 0.025% Bromophenol Blue, 0.025% xylene cyanol, 5 mM EDTA, 90% formamide and loaded onto a 10% sequencing PAGE with 6 M urea.

Curve fitting

A model summarized in Figure 6 (lower branch) and defined by two first-order rate constants k_{23} (rate to proceed from S2 to S3) and k_{34} (rate from S3 to S4) was found to fit the S2 and S3 data well (Supplemental Equations 4 and 5). PhosphorImager gel images were analyzed using ImageQuant V5.2 and then analyzed using Prism V software.

SUPPLEMENTAL MATERIAL

Supplemental material is available for this article.

ACKNOWLEDGMENTS

We thank D. Sen for critical comments concerning the manuscript. P.J.U. acknowledges funding from NSERC, MSFHR, and the SFU Community Trust Endowment Fund.

Author contributions: S.S.S.P. planned and performed experiments and contributed to preparation of the manuscript. P.J.U. planned experiments and contributed to writing the manuscript.

Received June 7, 2012; accepted September 14, 2012.

REFERENCES

Barrick JE, Sudarsan N, Weinberg Z, Ruzzo WL, Breaker RR. 2005. 6S RNA is a widespread regulator of eubacterial RNA polymerase that resembles an open promoter. *RNA* **11:** 774–784.

Beckmann BM, Burenina OY, Hoch PG, Kubareva EA, Sharma CM, Hartmann RK. 2011. In vivo and in vitro analysis of 6S RNA-templated short transcripts in *Bacillus subtilis*. *RNA Biol* **8:** 839–849.

Beckmann BM, Hoch PG, Marz M, Willkomm DK, Salas M, Hartmann RK. 2012. A pRNA-induced structural rearrangement triggers 6S-1 RNA release from RNA polymerase in *Bacillus subtilis*. *EMBO J* **31:** 1727–1738.

Brownlee GG. 1971. Sequence of 6S RNA of *E. coli*. *Nat New Biol* **229:** 147–149.

Cavanagh AT, Sperger JM, Wassarman KM. 2012. Regulation of 6S RNA by pRNA synthesis is required for efficient recovery from stationary phase in *E. coli* and *B. subtilis*. *Nucleic Acids Res* **40:** 2234–2246.

Chen J, Darst SA, Thirumalai D. 2010. Promoter melting triggered by bacterial RNA polymerase occurs in three steps. *Proc Natl Acad Sci* **107:** 12523–12528.

Ederth J, Artsimovitch I, Isaksson LA, Landick R. 2002. The downstream DNA jaw of bacterial RNA polymerase facilitates both transcriptional initiation and pausing. *J Biol Chem* **277:** 37456–37463.

Gildehaus N, Neusser T, Wurm R, Wagner R. 2007. Studies on the function of the riboregulator 6S RNA from *E. coli*: RNA polymerase binding, inhibition of in vitro transcription and synthesis of RNA-directed de novo transcripts. *Nucleic Acids Res* **35:** 1885–1896.

Kapanidis AN, Margeat E, Ho SO, Kortkhonjia E, Weiss S, Ebright RH. 2006. Initial transcription by RNA polymerase proceeds through a DNA-scrunching mechanism. *Science* **314:** 1144–1147.

Kim KS, Lee Y. 2004. Regulation of 6S RNA biogenesis by switching utilization of both σ factors and endoribonucleases. *Nucleic Acids Res* **32:** 6057–6068.

Klocko AD, Wassarman KM. 2009. 6S RNA binding to $E\sigma^{70}$ requires a positively charged surface of σ^{70} region 4.2. *Mol Microbiol* **73:** 152–164.

Mukhopadhyay J, Kapanidis AN, Mekler V, Kortkhonjia E, Ebright YW, Ebright RH. 2001. Translocation of σ^{70} with RNA polymerase during transcription: Fluorescence resonance energy transfer assay for movement relative to DNA. *Cell* **106:** 453–463.

Murakami KS, Masuda S, Campbell EA, Muzzin O, Darst SA. 2002. Structural basis of transcription initiation: An RNA polymerase holoenzyme-DNA complex. *Science* **296:** 1285–1290.

Revyakin A, Liu C, Ebright RH, Strick TR. 2006. Abortive initiation and productive initiation by RNA polymerase involve DNA scrunching. *Science* **314:** 1139–1143.

Roberts JW, Shankar S, Filter JJ. 2008. RNA polymerase elongation factors. *Annu Rev Microbiol* **62:** 211–233.

Sharma UK, Chatterji D. 2010. Transcriptional switching in *Escherichia coli* during stress and starvation by modulation of σ activity. *FEMS Microbiol Rev* **34:** 646–657.

Sharma CM, Hoffmann S, Darfeuille F, Reignier J, Findeiss S, Sittka A, Chabas S, Reiche K, Hackermuller J, Reinhardt R, et al. 2010. The primary transcriptome of the major human pathogen *Helicobacter pylori*. *Nature* **464:** 250–255.

Shephard L, Dobson N, Unrau PJ. 2010. Binding and release of the 6S transcriptional control RNA. *RNA* **16:** 885–892.

Trotochaud AE, Wassarman KM. 2004. 6S RNA function enhances long-term cell survival. *J Bacteriol* **186:** 4978–4985.

Wassarman KM, Saecker RM. 2006. Synthesis-mediated release of a small RNA inhibitor of RNA polymerase. *Science* **314:** 1601–1603.

Wassarman KM, Storz G. 2000. 6S RNA regulates *E. coli* RNA polymerase activity. *Cell* **101:** 613–623.

Wurm R, Neusser T, Wagner R. 2010. 6S RNA-dependent inhibition of RNA polymerase is released by RNA-dependent synthesis of small de novo products. *Biol Chem* **391:** 187–196.

Zhilina E, Esyunina D, Brodolin K, Kulbachinskiy A. 2012. Structural transitions in the transcription elongation complexes of bacterial RNA polymerase during σ-dependent pausing. *Nucleic Acids Res* **40:** 3078–3091.